ApJ Letters, in press
Preprint typeset using LaTeX style emulateapj v. 14/09/00

THE EVOLUTION OF FIELD EARLY-TYPE GALAXIES TO $Z \sim 0.7$

[1]

Tommaso Treu
California Institute of Technology, Astronomy Department, 105-24, Pasadena, CA 91125
tt@astro.caltech.edu
AND

Massimo Stiavelli, S. Casertano
Space Telescope Science Institute, 3700 San Martin Dr., Baltimore, MD 21218
AND

Palle Møller
European Southern Observatories, Karl-Schwarzschild Str. 2, D85748, Garching bei München, Germany
AND

Giuseppe Bertin
Università degli Studi di Milano, Dipartimento di Fisica, Via Celoria 16, I20133, Milano, Italy
ApJ Letters, in press

ABSTRACT

We have measured the Fundamental Plane (FP) parameters for a sample of 30 *field* early-type galaxies (E/S0) in the redshift range $0.1 < z < 0.66$. We find that: *i)* the FP is defined and tight out to the highest redshift bin; *ii)* the intercept γ evolves as $d\gamma/dz = 0.58^{+0.09}_{-0.13}$ (for $\Omega = 0.3, \Omega_\Lambda = 0.7$), or, in terms of average effective mass to light ratio, as $d\log(M/L_B)/dz = -0.72^{+0.11}_{-0.16}$, i. e. faster than is observed for cluster E/S0 (-0.49 ± 0.05). In addition, we detect [OII] emission > 5Å in 22% of an enlarged sample of 42 *massive* E/S0 in the range $0.1 < z < 0.73$, in contrast with the quiescent population observed in clusters at similar z. We interpret these findings as evidence that a significant fraction of massive field E/S0 experiences secondary episodes of star-formation at $z < 1$.

Subject headings: galaxies: elliptical and lenticular, cD — galaxies: evolution —- galaxies: formation — galaxies: structure

1. INTRODUCTION

The Fundamental Plane (Djorgovski & Davis 1987; Dressler et al. 1987; hereafter FP) is a tight correlation between the effective radius (R_e), the effective surface brightness (SB_e), and the central velocity dispersion (σ)

$$\log R_{\rm e} = \alpha \log\ \sigma + \beta\ SB_{\rm e} + \gamma \qquad (1)$$

that is observed to hold for local early-type galaxies (E/S0). Under the assumption that E/S0 are homologous dynamical systems the FP can be interpreted in terms of a power law relation between mass (M) and mass-to-light ratio (M/L) (Treu et al. 2001b and references therein). In recent years, it has been found that a tight FP exists in clusters out to redshift $z = 0.83$ (van Dokkum & Franx 1996; Pahre 1998; Bender et al. 1998; Kelson et al. 2000). The modest evolution of the intercept γ and the tightness of the FP at $0.1 < z < 1$ can be explained in terms of passive evolution and an old age of the stellar populations in cluster E/S0. The absence of a dramatic evolution in the slopes α and β argues against the interpretation of the FP "tilt" resulting solely from a mass-age relation.

So far, most of the studies have been focused on the cluster environment. However, the population of galaxies in clusters is likely to evolve with redshift by accretion of field galaxies. Therefore, in order to obtain a complete and reliable picture, it is necessary to study the evolution of E/S0 both in clusters and in the field. In addition, hierarchical clustering models (e. g., Kauffmann 1996) predict the stellar populations of field E/S0 to be significantly younger than the ones of cluster E/S0. The effects of age differences are difficult to observe in the local Universe (Bernardi et al. 1998), when the typical population ages are large, but are greatly enhanced at intermediate redshift. For these reasons, we have embarked on a campaign aimed at measuring the evolution of the FP of *field* E/S0 with redshift. In previous papers (Treu et al. 1999; 2001a, b; hereafter T01a,b), we have analyzed a sample of 19 E/S0, finding that a tight FP exists in the field out to $z \approx 0.4$ and that the evolution of the intercept is marginally faster than in the clusters, indicating a marginally younger age for field galaxies (see also van Dokkum et al. 2001 and Kochanek et al. 2000).

Here we present results from a larger sample of 30 E/S0 extended to $z \sim 0.7$, increasing dramatically our sensitivity to differences between cluster and field environment, and show that field E/S0 evolve faster than cluster ones at the 95% CL. In addition, we report on the detection of [OII]3727 emission in a significant fraction of *massive* field E/S0 at intermediate redshift, which we interpret as evidence for secondary episodes of star-formation.

We assume the Hubble constant, the matter density,

[1] Based on observations collected at ESO (Paranal) under programmes 65.O-0446 and 66.A-0362, and with the NASA/ESA HST, obtained at STScI, which is operated by AURA, under NASA contract NAS5-26555.

and the cosmological constant to be respectively $H_0 = 50h_{50}$km s^{-1}Mpc^{-1} ($h_{50} = 1.3$ when necessary), $\Omega = 0.3$, and $\Omega_\Lambda = 0.7$.

2. SAMPLE SELECTION AND OBSERVATIONS

The sample of E/S0 was selected on the basis of Hubble Space Telescope (HST) images taken from the HST-Medium Deep Survey (MDS; Griffiths et al. 1994). The selection criteria are identical to the ones extensively discussed in T01a, except for the color cut ($1.25 < V_{606}$-I_{814}, chosen to select higher redshift E/S0; V_{606} and I_{814} indicate Vega magnitudes through HST filters F606W and F814W respectively) and the magnitude range ($19.3 < I_{814} < 20.3$). The effects of color and magnitude selection are taken into account in the analysis presented here as discussed in T01b. Images are available at the MDS web site at http://www.archive.stsci.edu/mds. Morphological classification was performed independently by two of us (TT, MS), based on visual inspection of the images, of the residuals from the fit, and of the luminosity profiles. In particular, since contamination from Sa galaxies[2] could bias our results towards a younger age of the stellar populations, we were extremely conservative in rejecting galaxies that showed sign of a spiral disk either in the direct images (F606W and F814W), or in the residuals from the $r^{1/4}$ fit. As independent check of our classification, the bulge-to-total luminosity ratio measured by the MDS group for our E/S0 is always larger than 0.6 and typically in the range 0.8-1.

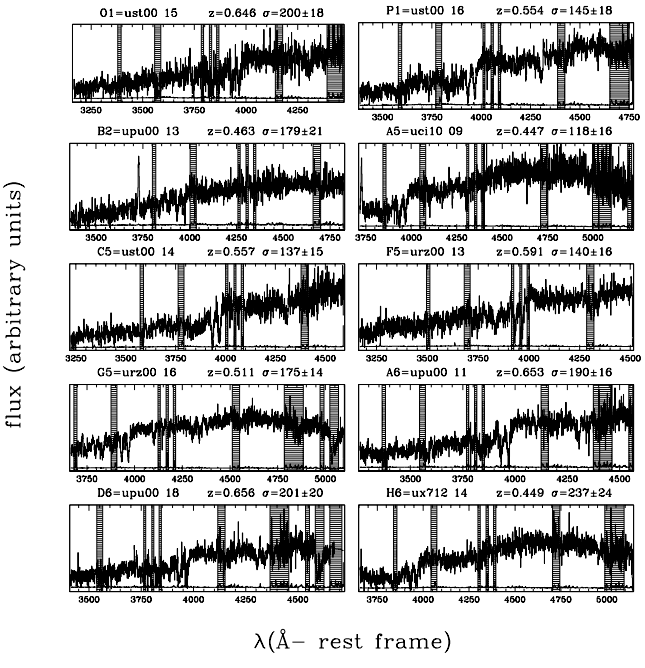

FIG. 1.— Spectra of galaxies with measured central velocity dispersion. The shaded regions are affected by sky-line residuals and atmospheric absorption and have been masked out during the fit. Note [OII] in emission in galaxies **B2** and **A5**.

Spectra for 16 galaxies were obtained in service mode from April 2000 to March 2001, using the Focal Reducer and Spectrograph 2 (FORS2) at the Very Large Telescope (VLT). The adopted grism R600 with a 1″ wide slit gives a resolution of $\sim 90 - 100$km s^{-1}; exposure times ranged between 2×1800s and 2×3600s. For 10 out of 16 E/S0 observed (Figure 1) we obtained a reliable central velocity dispersion (the success rate depending on observing conditions and redshift, since the observed wavelength range was optimized for the range $z \approx 0.45 - 0.65$). The data reduction was very similar to the one described in T01a. Combined with the data of T01b, our total sample consists of 42 galaxies (in the range $z = 0.10 - 0.73$), 30 of which with measured velocity dispersion ($z = 0.10 - 0.66$).

3. THE EVOLUTION OF THE FUNDAMENTAL PLANE

Panels (a) to (e) in Figure 2 show the location in the FP-space of the galaxies in our sample, binned in redshift. The data (open symbols) in the rest-frame B band[3] are compared to the local relation shown as solid line. The main result is that the brightening at fixed σ and R_e increases with redshift. By assuming constant slopes α and β we obtain the average evolution of the intercept with redshift plotted as filled pentagons in panel (f).

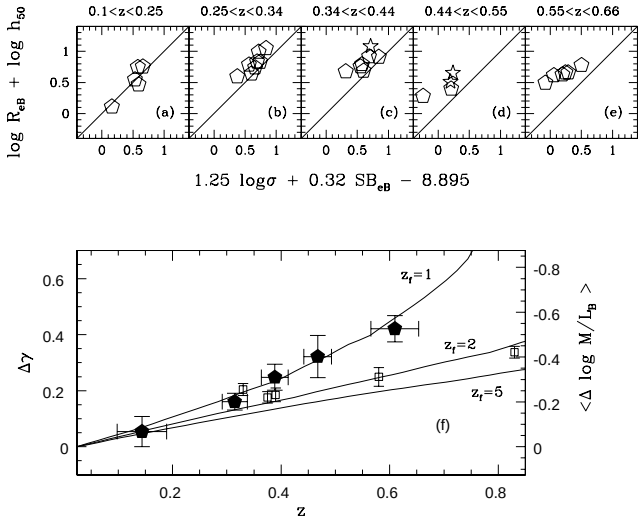

FIG. 2.— FP in the rest-frame B band. In panels (a) to (e) we show the field E/S0 (open stars if [OII] emission is detected, open pentagons otherwise), binned in redshift and compared to the FP found in the Coma Cluster (Bender et al. 1998). Panel (f) shows the average offset of the intercept of field galaxies from the local FP relation as a function of redshift (large filled pentagons), compared to the offset observed in clusters (open squares; van Dokkum & Franx 1996; Kelson et al. 1997; Bender et al. 1998; van Dokkum et al. 1998; Kelson et al. 2000). The solid lines represent the evolution predicted for passively evolving stellar populations formed in a single burst at $z = 1, 2, 5$ (from top to bottom) computed using Bruzual & Charlot (1993) models in the BC96 version (as described in T01b). We assume $\Omega = 0.3$, $\Omega_\Lambda = 0.7$ and $h_{50} = 1.3$

Under the assumption of passive evolution and constant slopes (T01b), the evolution of γ can be converted into the evolution of the average M/L ratio, which can be read on the right scale of panel (f). Modelling the evolution as $\gamma(z) = \gamma(0) + \gamma'(0)z$, where the prime indicates derivative with respect to z, a least χ^2 fit yields $\gamma'_B = 0.64$. However, in order to avoid biased results, it is crucial to take into account the selection process, for example by applying the Montecarlo-Bayesian method introduced in T01b, generalized by allowing the scatter to vary as a function

[2] See, e.g., Smail et al. (1997) and van Dokkum et al. (1998a) for a discussion.

[3] The analysis in the V band, or using different Coma FP, yields the same results, see T01b for discussion.

of redshift, $\sigma_\gamma(z) = \sigma_\gamma(0) + \sigma'_\gamma(0)z$. In this way, we derive the posterior probability density given the set of observations, $p(\gamma', \sigma'_\gamma|\{\gamma_i\})$ in the notation of T01b, shown in Figure 3 panel (a). The posterior probability peaks at $\gamma'_B = 0.58$ ($0.45 - 0.67$ 68% limit), which corresponds to $\log(M/L_B)' = -0.72^{+0.11}_{-0.16}$. The scatter is constant or at most mildly increasing with redshift. Note that the effects of the magnitude selection limit (see T01b) on the measured evolution of the intercept depend on the intrinsic scatter of the FP, and therefore it is important to study the combined probability density. Note also that the galaxies with OII emission (open stars in panels c and d) fall slightly above the quiescent ones (pentagons), as expected if their M/L is smaller because of a fraction of young stars. However, they do not dominate the general trend, since the results change very little if they are removed from the sample (e.g. γ'_B from the least χ^2 fit goes from 0.64 to 0.61).

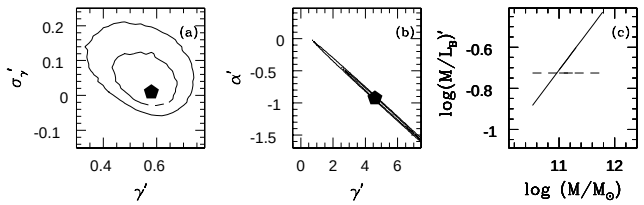

FIG. 3.— Panel (a): probability contours for the variation of the intercept and scatter with redshift (respectively γ' and σ'_γ; the pentagon marks the peak of the probability density, the dashed line the 68% limit and the solid line the 95% limit). Panel (b): probability contours for the variation of the intercept (γ') and slope (α') with redshift, obtained by assuming $\alpha' = 10\beta'$; symbols as in panel (a). Panel (c): evolution of M/L_B as a function of M (defined as $5\sigma^2 R_e/G$), as obtained by assuming fixed slopes (dashed line), or the values of α' and β' corresponding to the peak of the probability density in panel (b; solid line).

It is desirable to generalize the treatment by allowing also the slopes to evolve with redshift. Even though a larger sample is needed to this aim, possibly spanning a wider range of parameters, we will try to address this issue by assuming two additional constraints: *i)* the scatter does not change from $z = 0$ to $z \sim 0.7$ and *ii)* $\alpha' = 10\beta'$ (hence the FP is equivalent to a relation between M and M/L at any redshift). Under these assumptions, we obtain the results shown in Fig. 3 panels (b) and (c), plotted using $M = 5\sigma^2 R_e/G$ (Bender, Burstein & Faber 1992). The evolution of the slopes remains highly unconstrained (panel b), but the evolution of the M vs M/L relation is better constrained (panel c). For the typical masses in our sample ($< \log M/M_\odot >= 11.4$) the derived value of M/L' does not depend significantly on the value of α', providing a test of the robustness of the measurement. On the other hand, the result shown as a solid line in panel (c) would indicate that the evolution of M/L with redshift becomes slower as the mass increases (i.e. for example massive E/S0 are older). More data are needed to confirm these findings.

In Figure 2 we also show the evolution of γ predicted by assuming passively evolving single stellar populations. The best-fitting single burst redshift of formation should be interpreted in terms of a luminosity weighted redshift of formation, since it is clear that a more complex scenario than passive evolution of single coeval stellar populations is needed to explain the present observations (T01b). Finally, cluster data taken from the literature are shown as open squares in Figure 2 for comparison. The field FP evolves faster than the cluster one: for the cluster van Dokkum et al. (2001) measure $\log(M/L_B)' = -0.49 \pm 0.05$, i. e. $\gamma' = 0.39 \pm 0.04$, which falls on the 95% contour in panel (a) of Figure 3.

4. EMISSION LINE PROPERTIES

At $z \gtrsim 0.3$ the emission line [OII]3727 is redshifted into the wavelength range covered by our instrumental setup. Six out of 27 E/S0 for which [OII] is detectable show significant emission (rest-frame equivalent width EW$>$ 5 Å). If attributed to star-formation, the observed [OII] EW correspond to star-formation rates of order 0.5–5 $M_\odot/yr$ (Kennicutt 1992). The fraction of E/S0 with sizable star-formation in our sample is significantly larger than the one found for massive E/S0 in clusters at similar redshifts and in the local Universe. In Figure 4 we plot the fraction of E/S0 with [OII] EW$>$ 5 Å as a function of redshift for field (pentagons) and cluster (squares) samples taken from the literature.

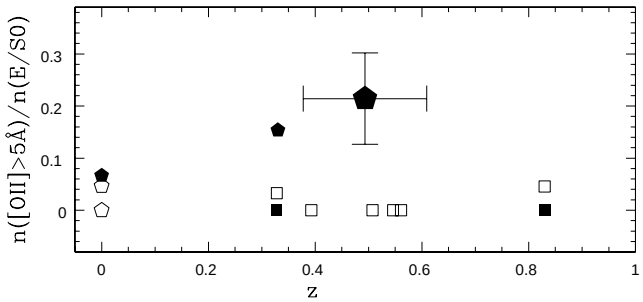

FIG. 4.— Fraction of E/S0 with [OII] emission larger than 5 Å EW (rest-frame) as a function of redshift. Pentagons represent field galaxies, squares cluster galaxies. The points are filled if selected similarly to our sample. Field galaxies are from Caldwell (1984), Kennicutt (1992), Jansen et al. (2000; limited to $M_B - 5\log h_{50} < -20$, corresponding roughly to our survey), Brinchmann et al. (1998; limited to $I_8 < 20.3$), and the present work (large filled pentagon with error bars). The filled squares are from Fisher et al. (1998), van Dokkum et al. (1998a), van Dokkum et al. (2000). The open squares are from Smail et al. (1997) and Dressler et al. (1999).

E/S0 with similar [OII] EW, or similarly with relatively blue colors, have been reported previously, suggesting that secondary episodes of star-formation are common at intermediate redshift (Schade et al. 1999; Menanteau et al. 2001). Im et al. (2001) measured the width of the [OII] line for a sample of blue E/S0 at intermediate redshift finding velocity dispersions $\sigma \lesssim 80$ kms^{-1}; based on this measurement they argue that most blue E/S0 are not the progenitors of present-day massive E/S0, but rather less massive spheroids, for which star-formation is observed also in the local Universe (Jansen et al. 2000). Our sample adds further information, because it is made of bright ($I < 20.3$) and *massive* E/S0. The velocity dispersions we obtained via absorption-line kinematics are typical of massive field E/S0. In particular, the three objects with significant [OII] emission for which velocity dispersion is available have $\sigma = 118, 179, 233$ km s^{-1}. From the FP relationship, as measured from our sample, we estimate for the other three galaxies with [OII] emission $\sigma = 105, 171, 261$

kms^{-1}.

We can estimate the amount of stellar mass assembled in these secondary burst in the following way. The probability of observing a burst is given by

$$p(\mathrm{OII}) = \bar{n}\frac{\bar{t}}{\Delta t}, \quad (2)$$

where $\bar{n}$ is the average number of bursts per galaxy, $\bar{t}$ is the average duration of the burst, and Δt is the interval in cosmic time between $z = 0.73$ and $z = 0.26$ when the burst was observable. The total average mass in secondary bursts is then:

$$M_{\mathrm{OII}} = \bar{n}\bar{t}\dot{\bar{M}} = p(\mathrm{OII})\Delta t\dot{\bar{M}}. \quad (3)$$

By using the observed values for $p(\mathrm{OII}) = 6/27$ and $\dot{\bar{M}} = 0.5 - 5 M_{\odot}\mathrm{yr}^{-1}$, we estimate that the average stellar mass formed in these bursts is of the order of $M_{\mathrm{OII}} \sim 5 \cdot 10^8 - 5 \cdot 10^9 M_{\odot}$.

5. CONCLUSIONS

Our sample of 30 field E/S0 defines a tight FP out to $z = 0.66$, with no or modest increase of the scatter with redshift. The intercept γ evolves with redshift as $\gamma' = 0.58$, which, interpreted in terms of passive evolution of the stellar populations, implies $\log(M/L_B)' = -0.72^{+0.11}_{-0.16}$, i.e. faster than that observed in clusters by other groups (e.g. -0.49 ± 0.05 van Dokkum et al. 2001). In addition, 22% of the galaxies show [OII] in emission, with $EW > 5$Å. Assuming the emission is due to star-formation, we estimate that such bursts produce of order $M_{\mathrm{OII}} \sim 5{\cdot}10^8{-}5{\cdot}10^9 M_{\odot}$ of stellar mass between $z = 0.73$ and $z = 0.26$.

The existence and tightness of the FP suggest that no major structural changes occur between $z \sim 0.7$ and $z = 0$. However, we find evidence that some stellar mass is formed at relatively recent time during secondary bursts. Although these bursts contribute only a small fraction of the total stellar mass they contribute significantly to the evolution of the observable luminous component. For example, a scenario where most of the stars formed at $z > 1$ and secondary star-formation occurs at $z < 1$ could not only explain the evolution of the FP (T01b) and the observed [OII] emission but could also reconcile the modest evolution of the number density of E/S0 observed to $z \sim 1$ (Schade et al. 1999; Im et al. 2001, in press), with the paucity of *red* E/S0 observed in some infrared surveys (Menanteau et al. 1999; Treu & Stiavelli 1999; see also Jimenez et al. 1999 and Daddi et al. 2000).

This research was supported by STScI grant AR-09222. We acknowledge the use of the Gauss-Hermite Fourier Fitting Software developed by R. van der Marel and M. Franx and useful conversations with A. Benson, R. Ellis, F. Menanteau, and P. van Dokkum.

REFERENCES

Bender, R., Burstein D., Faber, S. M. 1992, ApJ, 399, 462
Bender, R., Saglia, R. P., Ziegler, B., Belloni, P., Greggio, L., Hopp, U., Bruzual, G., 1998, ApJ, 493, 529
Bernardi M., Renzini A., da Costa L. N., Wegner G., Alonso M. V., Pellegrini P.S., Rité C., Wilmer C. N. A., 1998, ApJ, 508, L43
Brinchmann, J. et al. 1998, ApJ, 499, 112
Bruzual A. G., Charlot S., 1993, ApJ, 405, 538
Caldwell, N. 1984, PASP, 96, 287
Daddi, E., et al. 2000, A&A, 361, 535
Djorgovksi S. G., Davis M., 1987, ApJ, 313, 59
Dressler, A., Lynden-Bell, D., Burstein, D., Davies, R. L., Faber, S. M., Terlevich, R, Wegner G. 1987, ApJ, 313, 42
Dressler A., Smail I. R., Poggianti, B., Butcher, H., Couch W. J., Ellis R. S., Oemler A. 1999, ApJS, 122, 51
Fisher, D., Fabricant, D., Franx, M., van Dokkum, P. G. 1998, ApJ, 498, 195
Griffiths E. et al. 1994, ApJ, 435, L19
Im, M., Faber, S. M., Koo, D. C., Phillips, A. C., Schiavon, R. P., Simard, L. & Willmer, C. N. A., 2001, ApJ, in press
Jansen, R. A., Fabricant, D., Franx, M., Caldwell, N. 2000, ApJS, 126, 331
Jimenez, R., Friaca, A., Dunlop, J. S., Terlevich, R.J., Peacock J. A., Nolan, L. A., 1999, MNRAS, 305, L16
Kauffmann, G. 1996, MNRAS, 281, 478
Kennicutt R., 1992, ApJ, 388, 310
Kochanek, C. S. et al. 2000, ApJ, 543, 131
Kelson D. D., Illingworth G. D., van Dokkum, P. G. & Franx, M. 2000, ApJ, 531, 184
Kelson, D. D., van Dokkum, P. G., Franx, M., Illingworth G. D., & Fabricant, D. G. M. 1997, ApJ, 478, L13
Menanteau, F., Ellis, R. S. Abraham R. G., Barger A. J., Cowie L. L., 1999, MNRAS, 309, 208
Menanteau, F., Abraham, R. G., Ellis, R. S. 2001, MNRAS, 322, 1
Pahre, M. 1998, PhD Thesis, California Institute of Technology
Schade D. et al., 1999, ApJ, 525, 31
Smail I. R., Ellis R. S., Dressler A., Couch W. J., Oemler A., Sharples R. M. & Butcher H. ApJS, 1997, 479, 70
Treu, T. & Stiavelli, M., 1999, ApJ, 524, L27
Treu, T., Stiavelli, M., Casertano, C., Møller, P., & Bertin G. 1999, MNRAS, 308, 1307
Treu, T., Stiavelli, M., Møller, P., Casertano, C., & Bertin G. 2001a, MNRAS, 326, 221 [T01a]
Treu, T., Stiavelli, M., & Bertin G., Casertano, C., Møller, P. 2001b, MNRAS, 326, 237 [T01b]
van Dokkum P., Franx M., 1996, MNRAS, 281, 985
van Dokkum, P. G., Franx, M., Kelson D. D. & Illingworth G. D., 1998a, ApJ, 504, L17
van Dokkum, P. G., Franx, M., Kelson D. D. & Illingworth G. D., Fisher, D., Fabricant, D., 1998b, ApJ, 504, 714
van Dokkum, P. G., Franx, M., Fabricant, D., Illingworth, G. D., & Kelson D. D. 2000, ApJ, 541, 95
van Dokkum, P. G., Franx, M., Kelson D. D. & Illingworth, G. D., 2001, ApJ, 553, L39